Inorganic Chemistry

Communication

pubs.acs.org/IC

A Highly Stable 3D Acentric Zinc Metal−Organic Framework Based on Two Symmetrical Flexible Ligands: High Second-Harmonic-Generation Efficiency and Tunable Photoluminescence

Jin-Shuang Guo, Gang Xu, Xiao-Ming Jiang, Ming-Jian Zhang, Bin-Wen Liu, and Guo-Cong Guo*

State Key Laboratory of Structural Chemistry, Fujian Institute of Research on the Structure of Matter, Chinese Academy of Sciences, Fuzhou, Fujian 350002, People's Republic of China

Supporting Information

ABSTRACT: A 3D metal−organic framework (MOF), $[Zn(BPHY)(SA)]_n$ (**1**; BPHY = 1,2-bis(4-pyridyl)-hydrazine, H_2SA = succinic acid), which crystallizes in a noncentrosysmmetric space group (*Cc*), has been solvothermally obtained and testified to be a good nonlinear-optical material with the largest second-harmonic-generation response among the known MOFs based on sysmmetric ligands and high stability. Ultraviolet-to-visible tunable emission for **1** is observed.

Up to now, much effort has been devoted to exploring second-harmonic-generation (SHG) materials because of their practical importance in many areas, such as the laser industry and optoelectronic technologies.[1] As a result, numerous acentric SHG-active compounds have been obtained including organic, organometallic, inorganic, inorganic−organic hybrid complexes, and so on. Recently, metal−organic frameworks (MOFs) based on their superiorities in rational design and synthesis have become a hot research focus in the SHG field.[1f,2] The most direct way to construct acentric MOFs as promising SHG-active materials is introduction in unsymmetrical ligands, even chiral ligands. Although this is a traditional choice in the synthetic chemistry of SHG-active MOFs, it is, in fact, not the only option. As summed up by van der Veen et al, a noncentrosymmetric MOF could be obtained as long as the metal centers or metal clusters are coordinated in a non-centrosymmetric manner and organized in the network in such a way that there are no two clusters that are each other's inverse.[1f] Therefore, it is worth noting that noncentrosymmetric MOFs based on symmetrical ligands can be largely constructed according to the theory of van der Veen because symmetrical ligands have extremely plentiful species and can be synthesized much easier than nonsymmetrical and chiral ligands. However, so far the reported MOF materials constructed by symmetrical ligands with SHG efficiency are still very rare,[3] because there are still not enough practicable and effective strategies that are urgently needed for the construction of noncentrosymmetric MOFs based on symmetrical ligands.[4]

Our group has studied for a long time second-order nonlinear-optical (NLO) materials, and many significant results have been obtained.[5] In the most recent, aiming at full utilization of symmetrical ligands to construct novel acentric MOFs with excellent SHG performances, we are enlightened by the valuable study on supramolecular stereoisomerism[3c] and propose a new strategy to remove the inversion center for constructing noncentrosymmetric polar packing, that is, in situ capturing and using an unsymmetrical conformation of symmetrically flexible ligands in the crystallization process of MOFs. Flexible ligands usually can afford good plasticity and diversified conformations to establish MOFs, mostly because of the rotation of a single bond.[6] So, we choose a synthesis system of Zn^{II} and two flexible symmetrical ligands, 4,4′-azobispyridine (AZPY) and succinic acid (H_2SA), to verify the feasibility of our synthetic strategy. Successfully, a 3D acentric zinc MOF, $[Zn(BPHY)(SA)]_n$ [**1**; BPHY = 1,2-bis(4-pyridyl)hydrazine], which displays great performance as a second-order NLO material with large SHG efficiency and high stability, has been synthesized. In addition, MOF **1** also presents very interesting ultraviolet-to-visible tunable luminescence properties. Herein, we report the synthesis, structure, and optical properties of MOF **1**.

MOF **1** can be synthesized through the solvothermal reaction of $Zn(NO_3)_2{\cdot}6H_2O$, AZPY, and H_2SA in an *N*,*N*-dimethylformamide/H_2O (1:1, v/v) mixed solvent in the temperature range of 100−130 °C for 1 day, which can in situ reduce AZPY to a BPHY ligand and provides more opportunities for flexible BPHY and SA ligands to assume different configurations through changes in the reaction conditions.[7] Powder X-ray diffraction (PXRD; Figure S1 in the Supporting Information, SI) and elemental analysis indicate that the products are phase-pure.

Single-crystal X-ray diffraction analysis reveals that MOF **1** crystallizes in the noncentrosymmetric space group *Cc*. The asymmetric unit of **1** comprises one Zn^{II} ion, one BPHY ligand, and one SA ligand (Figure 1a). Each Zn^{II} ion is surrounded by two N atoms [Zn1−N1 2.029(2) Å; Zn1−N4 ($x - {}^1/_2, y - {}^1/_2, z - 1$) 2.044(3) Å] from two μ_2-BPHY ligands and two O atoms [Zn1−O1 1.977(3) Å; Zn1−O4 ($x - {}^1/_2, -y + {}^1/_2, z - {}^1/_2$) 1.960(2) Å] from two μ_2-κ_2-O1:O4 SA ligands, giving a distorted tetrahedral geometry, which lacks a center of symmetry to give out a polar ZnO_2N_2 center (Figure 1b). These polar centers are connected by BPHY and SA ligands both with unsymmetrical conformations to afford a 3D acentric MOF with a topology of 6.6.6.6.6(2). The Zn···Zn separations are 10.812(1) and 7.0575(9) Å spanned by BPHY and SA, respectively (Figure S3a−c in the SI). Owing to single-bond rotation of NH−NH and CH_2−CH_2 bonds within 360°, infinite conformations of BPHY and SA theoretically should exist, of which several typical

Received: February 9, 2014
Published: April 14, 2014

   dx.doi.org/10.1021/ic500315z | *Inorg. Chem.* 2014, 53, 4278−4280

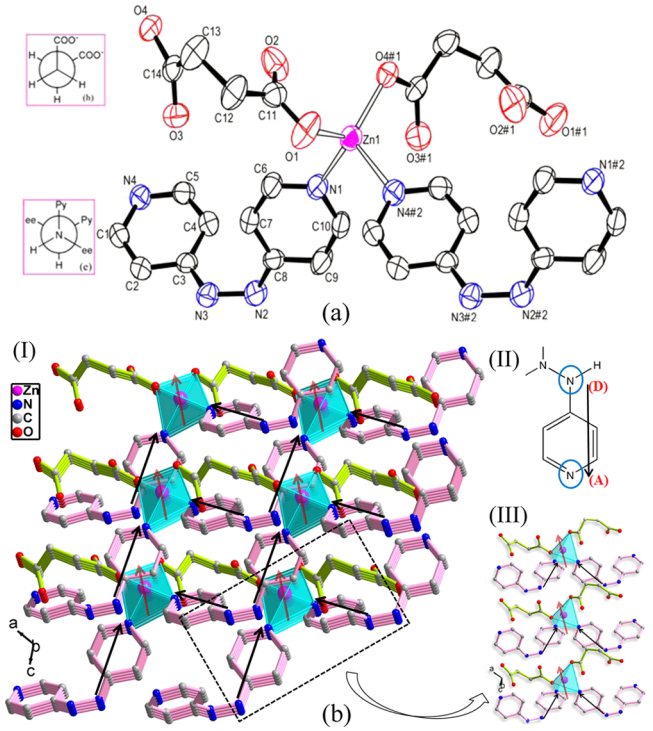

Figure 1. (a) Coordination environment around the Zn^{II} ion in **1** and conformations of BPHY and SA. H atoms have been omitted for clarity. Symmetry codes: #1, $x-{}^1/_2, -y+{}^1/_2, z-{}^1/_2$; #2, $x-{}^1/_2, y-{}^1/_2, z-1$. (b) Dipoles in **1**. Red and black arrows represent dipoles of distorted ZnO_2N_2 tetrahedra and BPHY ligands, respectively.

conformations are shown in Scheme S2 in the SI. In MOF **1**, the BPHY ligand adopts an unsymmetrical conformation with a C8−N2−N3−C3 torsion angle of 94.9(3)°, which is much larger than the ideal torsion angle (60°) in the conformation (e), while the SA ligand with a C11−C12−C13−C14 torsion angle of 61.0(4)° displays an unsymmetrical conformation (h). There are mainly two reasons for the successful construction of MOF **1** to be an acentric structure. First, two types of coordinating atoms occupy four vertexes of tetrahedral geometry, resulting in non-centrosymmetric ZnO_2N_2 centers. Second, symmetrical flexible ligands show an unsymmetrical linkage between ZnO_2N_2 centers via the rotation of single bonds.

Because MOF **1** has an acentric structure, the SHG measurements have first been carried out and obtained a satisfactory result. A sample of KH_2PO_4 (KDP; 100−150 μm) was prepared as a reference material. The SHG efficiency of **1** is 11.5 times that of KDP. The second-order susceptibility $\chi^{(2)}_{eff}$ of a KDP powder sample is about 0.36 pm/V, so the derived second-order susceptibility $\chi^{(2)}_{eff}$ for **1** is 4.14 pm/V (9.88×10^{-9} esu), which is stronger than many acentric MOFs constructed from chiral ligands.[3a] As shown in Figure 2, the SHG signals as a function of the particle size made on ground crystals of **1** suggest that its phase-matching property is type I.[8]

The calculated band gaps of **1** using the local density approximation are E_g = 3.20 eV (Figure S4a in the SI), which is smaller than the experimental value 3.80 eV (Figure S5 in the SI). So, the scissor operator of 0.6 eV is obtained for calculations of the optical properties of **1**.

The calculated imaginary part $\varepsilon_2(\omega)$ and real part $\varepsilon_1(\omega)$ of the frequency-dependent dielectric functions of **1** are shown in Figure S6 in the SI. The space group of **1** belongs to class *m* and has 10 nonvanishing independent second-order susceptibility

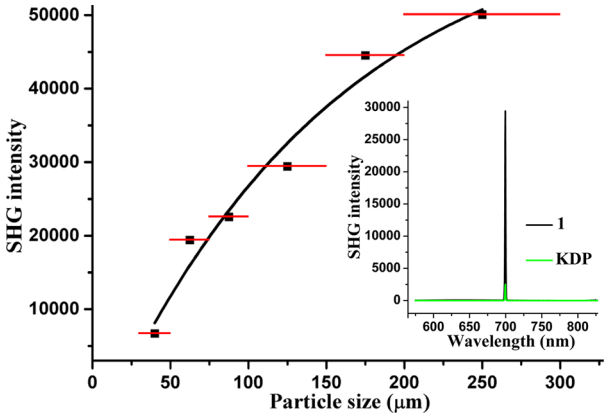

Figure 2. Phase-matching results for **1**. Inset: SHG signals of **1** and KDP.

tensors ($\chi_{111}, \chi_{122}, \chi_{133}, \chi_{113}, \chi_{223}, \chi_{212}, \chi_{311}, \chi_{322}, \chi_{333}$, and χ_{313}). In the low-energy region and under the restriction of Kleinman's symmetry, only six independent SHG tensors (χ_{111}, χ_{122}, χ_{133}, χ_{113}, χ_{223}, and χ_{333}) remain. The calculated χ_{111}, χ_{122}, χ_{133}, χ_{113}, χ_{223}, and χ_{333} at a wavelength of 1400 nm (0.89 eV) are 1.27×10^{-9}, 1.15×10^{-9}, 2.00×10^{-9}, 1.59×10^{-9}, 1.51×10^{-9}, and 2.66×10^{-9} esu, respectively (Figure S7 in the SI). The calculated average second-order susceptibility $\chi^{(2)}_{ave}(2\omega,\omega,\omega)$ defined as $(1/6)\sum\chi^{(2)}_{ij}(2\omega,\omega,\omega)$ is 1.70×10^{-9} esu, which is on the same order as our experimentally derived $\chi^{(2)}_{eff}$ coefficient for **1** (9.88×10^{-9} esu). The large SHG response of **1** is attributed mainly to the electronic asymmetry enhanced by a synergistic effect of the donor−acceptor (D−A) system of −NHPy groups (Py = pyridyl) and polarization of ZnO_2N_2 centers (Figure 1b). In detail, the imino group (−NH−) participates as an electron-donating group for the Py ring, which is an accepted group; in the meantime, coordination of the Py ring to the Zn^{II} center results in a N atom of Py donating the lone pair of electrons to the metal center and the formation of another excellent D−A system.[9] Moreover, the existence of a coordinated carboxyl group further enhances the effect of electron-withdrawing. It is well-known that the SHG responses depend on the charge separation or molecular dipolar moment (hyperpolarizability); the whole polar $Zn(NHPy)_2(COO)_2$ group with conjugated D−A systems whose polarization is intensified by metal−ligand coordination could be responsible for the strong enhancement of the SHG response of **1**. Besides, the choice of Zn^{II} in this MOF is not only for its contribution to building polar ZnO_2N_2 groups but also for avoiding unwanted d−d transitions in the visible region.[2b]

Furthermore, no solvent molecule is found in **1**. The TGA results show that MOF **1** decomposes at ∼330 °C (Figure S8 in the SI), and there is no phase transition observed before decomposition, as suggested by the DSC curve. The high stability of **1** further makes it to be a good SHG material with a relatively high laser damage threshold.

The solid-state luminescence of **1** was in situ investigated with the excitation light variation varying at room temperature, and the results show that, when MOF **1** was excited by variation of light in the range of 325−340 nm, it exhibited tunable Ultraviolet-to-visible photoluminescence from 390 to 445 nm. There are three typical stages for the whole luminescence process of **1**, as shown in Figure 3. First excited at 300−325 nm, MOF **1** displays a maximum emission at 390 nm with a maximum excitation light of 322 nm. Then as the excitation light shifts to long wavelength, the 390 nm peak of the emission spectrum becomes lower and simultaneously the intensity at ∼445 nm

dx.doi.org/10.1021/ic500315z | Inorg. Chem. 2014, 53, 4278−4280

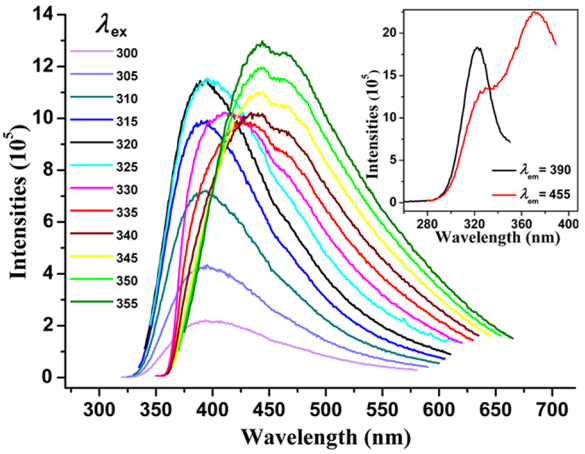

Figure 3. Solid-state emission spectra of **1** by variation of the excitation light under the same conditions. Inset: excitation spectra (ex = excitation, em = emission).

increases. Upon excitation at 340−355 nm, the emission peak at 445 nm is observed because the maximum emission for 1 and 370 nm is found to be the maximum excitation light for this peak.

Theoretical calculation on the structure of **1** by evaluation of the density of states (DOS) is helpful to better understanding the photoluminescent mechanism.[10] On the basis of the theoretical results for **1** (Figure S4b in the SI), the top of the valence bands (VBs) between energy −2.2 and 0.0 eV is dominated by a mixture of p−π orbitals of the carboxyl and Py groups provided by SA and BPHY ligands, respectively. The bottom of the conduction bands is almost contributed by the p−π* antibonding orbital of the Py group. Theoretically, BPHY-centered and SA-to-BPHY charge transfer coexist in the absorption transition of **1**. It is reasonable to attribute the emission peaks at 390 and 445 nm to the π−π* transition of BPHY and intergroup π−π* transitions between SA and BPHY, respectively. Furthermore, p−π orbital of the Py group makes relatively more contribution than that of the carboxyl group in the low-energy region of the VBs, while that of the carboxyl group contributes more in the high-energy region. Accordingly, from energy −2.2 to 0.0 eV, the proportion of the intergroup π−π* transition becomes greater. As a result, an increase of the excitation wavelength (range from 325 to 340 nm) gradually enhances the intensity of the 445 nm peak and lowers that of the 390 nm peak, which confirms **1** to be a typical tunable luminescent material with a tuning range of 390−445 nm.[11]

In summary, a novel 3D acentric MOF **1**, as an excellent NLO material exhibiting large SHG efficiency and highly thermal stability, has been prepared using symmetrically flexible ligands that can afford unsymmetrical conformations to be suitable for the construction of an acentric structure. Meanwhile, MOF **1** can be adjusted to show ultraviolet-to-visible tunable photoluminescence benefiting from the mixed-ligand strategy. The high SHG efficiency and tunable photoluminescence of **1** have been explained by theoretical calculations of second-order NLO susceptibility and DOS. Our synthesis from symmetrical ligands to acentric MOFs opens a valuable avenue for obtaining good NLO materials, and there must be a wider research field of acentric MOFs constructed by symmetrical ligands.

■ ASSOCIATED CONTENT

Supporting Information

Schematic in situ reduction, PXRD, FT-IR, UV diffuse-reflectance and absorption spectra, TGA, DSC, additional structural plots, and X-ray crystallographic file in CIF format. This material is available free of charge via the Internet at http://pubs.acs.org.

■ AUTHOR INFORMATION

Corresponding Author

*E-mail: gcguo@fjirsm.ac.cn.

Notes

The authors declare no competing financial interest.

■ ACKNOWLEDGMENTS

We gratefully acknowledge financial support by the NSF of China (Grants 21103188, 21101152, and 21221001), National Key Technology R&D Program (Grant 2012BAE06B08), Key Project from the CAS (Grant KJCX2-EW-H03), and the NSF of Fujian Province (Grant 2011J06006).

■ REFERENCES

(1) (a) Chen, C.; Liu, G. *Annu. Rev. Mater. Sci.* **1986**, *16*, 203−243. (b) Nalwa, H. S. *Appl. Organomet. Chem.* **1991**, *5*, 349−377. (c) Marder, S. R.; Perry, J. W.; Yakymyshyn, C. P. *Chem. Mater.* **1994**, *6*, 1137−1147. (d) Burland, D. *Chem. Rev.* **1994**, *94*, 1−2. (e) Fiebig, M.; Pavlov, V. V.; Pisarev, R. V. *J. Opt. Soc. Am. B* **2005**, *22*, 96−118. (f) van der Veen, M. A.; Verbiest, T.; De Vos, D. E. *Microporous Mesoporous Mater.* **2013**, *166*, 102−108.

(2) (a) Evans, O. R.; Lin, W. *Acc. Chem. Res.* **2002**, *35*, 511−500. (b) Wang, C.; Zhang, T.; Lin, W. *Chem. Rev.* **2012**, *112*, 1084−1104. (c) Yang, H.; Sang, R.-L.; Xu, X.; Xu, L. *Chem. Commun.* **2013**, *49*, 2909−2911.

(3) (a) Huang, S. D.; Xiong, R.-G.; Han, J.; Weiner, B. R. *Inorg. Chim. Acta* **1999**, *294*, 95−98. (b) Reinsch, H.; van der Veen, M. A.; Gil, B.; Marszalek, B.; Verbiest, T.; de Vos, D.; Stock, N. *Chem. Mater.* **2013**, *25*, 17−26. (c) Sun, D.; Collins, D. J.; Ke, Y.; Zuo, J.-L.; Zhou, H.-C. *Chem.—Eur. J.* **2006**, *12*, 3768−3776. (d) Chu, Q.; Liu, G.-X.; Huang, Y.-Q.; Wang, X.-F.; Sun, W.-Y. *Dalton Trans.* **2007**, 4302−4311.

(4) (a) Fang, Q.; Zhu, G.; Xue, M.; Sun, J.; Sun, F.; Qiu, S. *Inorg. Chem.* **2006**, *45*, 3582−3587. (b) Liu, J.-L.; Bao, X.; Leng, J.-D.; Lin, Z.-J.; Tong, M.-L. *Cryst. Growth Des.* **2011**, *11*, 2398−2403.

(5) (a) Zhou, W.-W.; Chen, J.-T.; Xu, G.; Wang, M.-S.; Zou, J.-P.; Long, X.-F.; Wang, G.-J.; Guo, G.-C.; Huang, J.-S. *Chem. Commun.* **2008**, *0*, 2762−2764. (b) Xu, G.; Li, Y.; Zhou, W.-W.; Wang, G.-J.; Long, X.-F.; Cai, L.-Z.; Wang, M.-S.; Guo, G.-C.; Huang, J.-S. *J. Mater. Chem.* **2009**, *19*, 2179−2183. (c) Jiang, X.-M.; Zhang, M.-J.; Zeng, H.-Y.; Guo, G.-C. *J. Am. Chem. Soc.* **2011**, *133*, 3410−3418.

(6) (a) Carlucci, L.; Ciani, G.; Proserpio, D. M.; Rizzato, S. *CrystEngComm* **2002**, *4*, 121−129. (b) Li, J.-R.; Bu, X.-H.; Zhang, R.-H.; Ribas, J. *Cryst. Growth Des.* **2005**, *5*, 1919−1932.

(7) Gai, Y.-L.; Jiang, F.-L.; Xiong, K.-C.; Chen, L.; Yuan, D.-Q.; Zhang, L.-J.; Zhou, K.; Hong, M.-C. *Cryst. Growth Des.* **2012**, *12*, 2079−2088.

(8) Kurtz, S. K.; Perry, T. T. *J. Appl. Phys.* **1968**, *39*, 3798−3813.

(9) (a) Ye, Q.; Li, Y.-H.; Song, Y.-M.; Huang, X.-F.; Xiong, R.-G.; Xue, Z. *Inorg. Chem.* **2005**, *44*, 3618−3625. (b) Gao, F.; Zhu, G.; Chen, Y.; Li, Y.; Qiu, S. *J. Phys. Chem. B* **2004**, *108*, 3426−3430.

(10) Wang, M.-S.; Guo, S.-P.; Li, Y.; Cai, L.-Z.; Zou, J.-P.; Xu, G.; Zhou, W.-W.; Zheng, F.-K.; Guo, G.-C. *J. Am. Chem. Soc.* **2009**, *131*, 13572−13573.

(11) Allendorf, M. D.; Bauer, C. A.; Bhakta, R. K.; Houk, R. J. T. *Chem. Soc. Rev.* **2009**, *38*, 1330−1352.